# Influence of Rock Microstructure on Rock Strength and Drilling Rate of Penetration (ROP)

Salum Mafazy, Michael Marsh, Zijian Li, & Stephen Butt
*Department of Process Engineering – Memorial University of Newfoundland, St. John's, NL, Canada*

GeoCalgary 2022 October 2-5
Reflection on Resources

ABSTRACT
During recent near-surface drilling operations to a measured depth of 90 m using both diamond core drilling and large diameter drilling, there was a marked decrease in drilling ROP over the depth interval, 50 - 55 m. A laboratory investigation was conducted, which included detailed core logging, rock mechanical tests, cuttings size analysis, and Mineral Liberation Analysis (MLA). Theoretical models were utilized and compared with field drilling performance metrics. It was observed that high rock strength in the mentioned interval and it is proposed that this caused the reduction in ROP. MLA application showed that the mineral composition remained constant, but the rock microstructure differed in that interval. Hence, alteration of microstructure may be the contributing factor that lead to increased rock strength and reduced ROP.

RÉSUMÉ
Au cours des récentes opérations de forage près de la surface à une profondeur mesurée de 90 m utilisant à la fois des forages au diamant et des forages à grand diamètre, il y a eu une diminution marquée de la ROP de forage sur l'intervalle de profondeur, 50 - 55 m. Une enquête en laboratoire a été menée, qui comprenait une diagraphie détaillée des carottes, des tests mécaniques de la roche, une analyse de la taille des déblais et une analyse de la libération des minéraux (MLA). Des modèles théoriques ont été utilisés et comparés aux mesures de performance de forage sur le terrain. Il a été observé que la résistance de la roche était élevée dans l'intervalle mentionné et il est proposé que cela ait causé la réduction de la ROP. L'application MLA a montré que la composition minérale restait constante, mais la microstructure de la roche différait dans cet intervalle. Par conséquent, l'altération de la microstructure peut être le facteur contributif qui conduit à une résistance accrue de la roche et à une ROP réduite.

## 1 INTRODUCTION

Large Diameter Hole (LDH) drilling is the method for drilling holes that can be considered greater than 50 cm in diameter for mining extraction. Such techniques are used for Tunnel Boring, Raise Boring, and Pile Drilling. Understanding the geometry, geological characteristics and properties of underground rock, such as lithology variation, Rock Quality Designation (RQD), etc., is essential for optimizing drilling performance and ultimately reducing drilling operation costs. The geological properties are typically obtained via core analysis prior to mining extraction (if desired). The analysis is needed to identify additional geological information and to determine the strength and hardness of the rock.

Drilling performance for most drilling operations is evaluated using the ROP metrics. Additionally, drilling parameters such as Revolution per Minute (rpm), Weight-on-Bit (WOB) and torque are also essential for the drilling performance of a well. Drilling optimization depends on these drilling performance parameters and hole cleaning efficiency. The higher the cleaning/drilling efficiency of a well, the higher the performance. Drilling efficiency depends on the specific energy required to penetrate the rock formation (Butt et al. 2016).

This study utilizes field trial LDH drilling (1 m) performance metrics and data. A notable reduction in ROP across a specific measured depth interval of 50 m to 55 m was observed. At the same time, no notable variation in above and/or below geological lithology was logged and any variation in drilling operating parameters was accounted for. The well was drilled through a mineral vein deposit (and host rock), inclined 30 degrees to the vertical and reached a measured depth of 90 m. This work aims to investigate the cause(s) of such abnormal drilling performance behavior. Laboratory experiments were performed for rock characterization, including core logging, rock strength testing, grain size distribution analysis, and Mineral Liberation Analysis (MLA).

### 1.1 Application of Tunnel Boring Machine (TBM) and Large Diameter Bit using Disc Cutters

In the study of mechanical rock crushing, several cutting methods are applied to mining equipment. The basic cutting methods can be categorized as drag bit cutting, point-attack bit cutting, disc cutting, button cutting, and roller cutting (Breeds et al. 1992). Disc cutters are used in drilling equipment like TBMs. TBMs were applied in mining in the late 1950s to 1970s. However, in recent years, there have been improvements in TBM design due to advancements in new technology and the use of computer system development (Cigla et al. 2001). For the field trial LDH drilling, a disc cutter bit arrangement was utilized. The disc cutters are mounted on a cutter head via independent bearing assemblies where the disc cutters are free to roll with respect to the thrust and drag force applied. Figure 1 shows a large diameter bit.

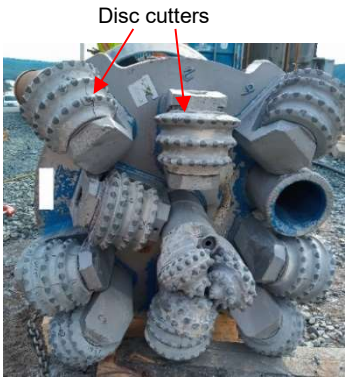


Figure 1. Large diameter bit (1 m)

## 1.2 Application of Core Logging

Diamond Drilling (DD) uses drill bits impregnated with fine to micro-fine industrial diamond crystals (Cumming & Smit, 1980). The drill bit is combined with the core barrel and attached to the drill string. The diamond bit cuts the rock column into a cylindrical shape known as the drill core. Usually, the core moves up into the drill pipe while the bit penetrates the rock (Abzalov, 2016). Once the drill core is recovered, it is placed in the core tray and stored in the core boxes. The application of drill core is widely used in engineering drilling, exploration of mineral deposits, geological boreholes, hydrogeological wells, and other underground drilling operations.

Core logging is the process of documenting key geological information to determine the lithology, mineralogy, geologic history and other geological parameters of a drilled location. Core logs also include wellbore logistic information such as the well location, wellbore number, etc.

RQD can be calculated from information recorded obtained from the logged core data. RQD is developed to provide an estimation of the quality of a rock mass for the drilled core. It is calculated as a percentage of intact core pieces longer than 10 cm in a total length of the core. It is a quick method applied in core logging applications, regardless it is limited to determine the rock mass quality for the core pieces less than ten centimeters (Palmstrom, 2005). Equation 1 defines the expression for calculating RQD and Table 1 expresses the grading of the RQD values.

$$RQD = \frac{\sum \text{Length (L)of core pieces>10 cm length}}{\text{Total length of the core run}} \quad [1]$$

Table 1. Rock quality designation (RQD) percentage and grading (Palmstrom, 2005).

| RQD (%) | Grade |
|---|---|
| 0 – 25% | Very poor |
| 25 – 50% | Poor |
| 50 – 75% | Fair |
| 75 – 90% | Good |
| 90 – 100% | Excellent |

## 1.3 Mechanical Tests Needed for Rock Characterization

Rock mechanical tests are used to obtain the mechanical parameters of a rock mass and help researchers / engineers to study different characteristics of rocks. For example, the various mechanical tests are utilized to determine Unconfined Compressive Strength (UCS), Indirect Tensile Strength (ITS), Point Load Strength Index (PLSI), Elastic Modulus, Poisson's Ratio, etc. Additionally, the determination of stress and strain of the rock under failure conditions will determine the strength, deformation, and stability characteristics of the tested rock.

In the area of rock characterization, researchers have conducted a tremendous amount of research and high achievements. Quan et al. 2021 conducted strength tests on granite and Rock-Like Materials (RLM) as concrete (isotropic rocks) and developed empirical correlations that describe the relationship between the UCS, ITS, and PLSI, between PLSI and ITS, and between P-wave and UCS, Young's modulus, and Poisson's ratio.

According to Quan et al. 2021 evaluated tensile and shear fracture on the sandstone samples for optimizing drilling performance using a roller cone bit and Polycrystalline Diamond Compact (PDC) Bit.

Also, Zhao et al. 2018, performed several laboratory mechanical tests to determine the damage characteristic of the rocks, and presented FLAC$^{3D}$ numerical simulation analyses to optimize the rock mechanical parameters obtained.

## 1.4 The Relationship between Cutting Size and Drilling Performance

Drill cuttings have been used in many applications involving mining and oil and gas drilling to determine the subsurface information. Mud loggers use drill cuttings to obtain information on lithology, and geological engineers need cuttings to understand rock properties such as porosity and permeability. Furthermore, cutting size distribution helps drilling operations improve drilling performance and prevent problems while drilling since they are associated with the drill bit, rock formation and fluid interaction (Karimi, 2013).

Cutting Size Analyses (CSA) is generally conducted to analyze drill cutting size parameters. The cuttings contain a variation in size ranges and there is a need to sort them from fine to course by using a standardized grain size distribution curve, which represents the size and weight composition of the particles. The detailed procedures and analysis followed (ASTM D6913/6913M, 2017).

## 1.5 Specific Energy and ROP Prediction Models

In rock excavation methods, the penetration of the drilling tool into the rock can be achieved by two main actions, 'indentation' in which the tooth of the bit is pushed into the rock to establish a bite; 'cutting' by which the bit gives lateral direction for breaking the rock into small pieces (Teale, 1965).

Generally, drilling energy is a key parameter for penetration by cutting the rock into small fragments.

Hence, drilling energy is used to characterize the drilling penetration and cuttings transportation process, known as Drilling Efficiency (DE). DE is defined as the energy consumed by the drilling process. Work done per unit volume excavated is known as specific drilling energy. The Mechanical Specific Energy (MSE) model is to analyze drilling efficiency.

Equation 2 presents the model for calculating MSE (Teale, 1965). Then according to Butt, 2016 shows the relation between DE, the strength of the rock penetrated and MSE as shown in Equation 3.

$$MSE = \frac{WOB}{A_B} + \frac{60*2\pi*NT}{A_B*ROP} \quad [2]$$

Where:

MSE = mechanical specific energy, Pa; N = rotary speed, rpm; $A_B$ = bit area, $m^2$; ROP = rate of penetration, m/h; T = torque, Nm; WOB = weight-on-bit, N

$$DE = \frac{CCS}{MSE} 100\% \quad [3]$$

Where:

CCS = in situ or confined compressive strength of the formation.

ROP is a result of the different drilling parameters such as rock strength variation, WOB applied, fluid circulation, etc. ROP models are used to predict the maximum WOB at any bit rotation and to observe the ROP variation for a given bit condition. The concept of the *'perfect cleaning*' in rotary drilling is one of the earlier invented ROP models, which means the tooth of the bit removes all the rock cuttings completely under the conditions presented in Equation 4 (Maurer, 1962):

$$R = \frac{k}{S^2}\left[\frac{W-W_o}{d_b}\right]^2 N \quad [4]$$

Where:

R = rate of penetration, m/h; k = calibration constant; S = in situ strength, MPa; W = weight on bit, kN; $W_o$ = threshold weight on bit, kN; $d_b$ = bit diameter, m; N= rotary speed, rpm

### 1.6 Mineral Liberation Analysis (MLA) Technology

MLA is the automated process that allows quantitative evaluation of mineral abundance, associations, sizes and shapes of minerals in a drill core sample in an automated systematic fashion. The advantage of using MLA is that it is a computer-automated system. It increases productivity with a better statistical representation when more samples are analyzed. MLA can analyze fine material at the scale of micrometers. Also, it gives a clear mapping of the mineral grain microstructure of the rock sample. However, MLA has difficulties distinguishing similar mineral compositions and polymorphs (Pszonka & Sala, 2018).

The MLA technology has been applied in many applications such as in the mineralogy and metallurgical processing industry, different studies of sediments and sedimentary rock, microstructure in mine tailings, etc. (Sylvester, 2012).

## 2 BACKGROUND

This paper utilizes field trial LDH drilling performance metrics and data. The field trial drilling occurred in a geological zone involving mainly quartz and mafic rock lithology. Drilling research was conducted throughout the vein (quartz) and host (mafic) lithology. A Diamond Diameter Hole (DDH) of NQ (47.6 mm) size was drilled before a LDH for the purpose of geologic evaluation.

An investigation for the specified interval to analyze the cause of low ROP was conducted. The core extracted from DDH was analyzed. Then, the elastic property, rock strength, and hardness tests were performed. Also, the rock's mineral composition was conducted using MLA technology.

Additionally, grain size analyses of the drill cuttings from the LDH were conducted. Then the cuttings size distribution parameters such as D10, D30, D50, D60, D90, Cu, and Cc correlated with drilling parameters to analyze the occurred phenomena.

Also, the ROP from the LDH was validated with the Maurer model, MSE, and the DE within the specified drilling interval.

### 2.1 Core Logging

Before the laboratory mechanical tests were performed, the drill cores from the DDH (intervals of 46.47 m to 55.3 m) were analyzed to identify lithology and RQD. Fig. 2 and Fig. 3 show the core boxes with their respective depth intervals. Table 2. Illustrates the relationship between interval depth, lithology type and corresponding RQD.

Figure 2. Core depth; 46.47 m to 51 m

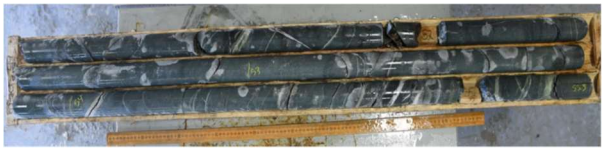

Figure 3. Core depth; 51 m to 55.3 m

Table 2. Core analysis for RQD and lithology

| Depth (m) | Identified Lithology | RQD | Grade |
|---|---|---|---|
| 46.5 m to 51 m | Mafic ash tuff with greyish-white color | 55.8% | Fair |
| 51 m to 55.3 m | Mafic ash tuff green-greyish color | 56.6% | Fair |

## 2.2 Sample preparation

Core samples were prepared for each of the selected mechanical tests. The sample preparation procedure started by the section of intact cores from each respective interval of interest and in turn, each sample was cut to a specified dimension as dictated by the ASTM standards.

## 2.3 Mechanical Tests

### 2.3.1 Strength Tests

In this study, UCS, PLSI, and ITS tests were performed on all test samples via the geomechanics loading frame. The frame has a maximum design load of 450 kN and is equipped with a Multi-sensor Data Management System including a Linear Variable Displacement Transducer (LVDT) and load cell. The LVDT measures the linear displacement of the tested sample. Also, a data acquisition (DAQ) is connected for the analog signal to digital conversion.

The sample preparation, testing procedures and calculations for the UCS, PLSI and ITS follow ASTM D7012, ASTM D5731, and ASTM D3967 standards, respectively. Figure 4 illustrates the experimental setup for the UCS and ITS test, which was performed using a flattened circular plate of a frame. Additionally, the PLSI test was performed using plates of the frame.

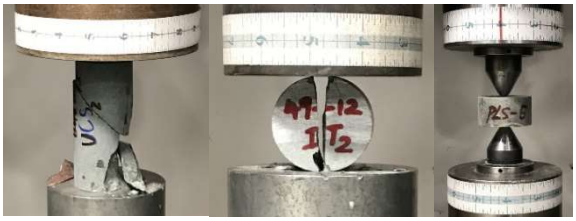

Figure 4. UCS (left), ITS (middle), and PLSI (right); experimental setup on the geomechanics frame

### 2.3.2 Hardness Test

A digital Schmidt hammer device was used to test rock hardness. The sample preparation and procedures follow ASTM D5873. For a digital device, the rebound hammer values are automatically normalized to the horizontal direction by setting up an angle, $\theta = 0°$ (Basu & Aydin, 2004). The test was performed at ten different positions on the rock core sample and the rebound values were recorded automatically.

## 3 RESULTS AND ANALYSIS

### 3.1 Drilling Parameters and ROP Models Analysis

Drilling parameter data from the LDH drilling field trials was recorded. The data was analyzed to determine the correlation between drilling parameters and varying lithology. More specifically, the variation between quartz, mafic ash tuff, and mafic massive flow. An unexpected low ROP can be observed in the mafic ash tuff interval between 50 m to 55 m. Figure 5 illustrates the correlation of WOB, ROP, and measured depth.

Later, the ROP was normalized using 20 rpm to remove the effect of rotary speed on the ROP. Normalized ROP was obtained from the actual ROP multiplied by the ratio of the rated rotary speed over the actual one (Xiao et al. 2015). The relationship between actual ROP, normalized ROP with depth, and WOB is shown in Fig. 6 and Fig. 7.

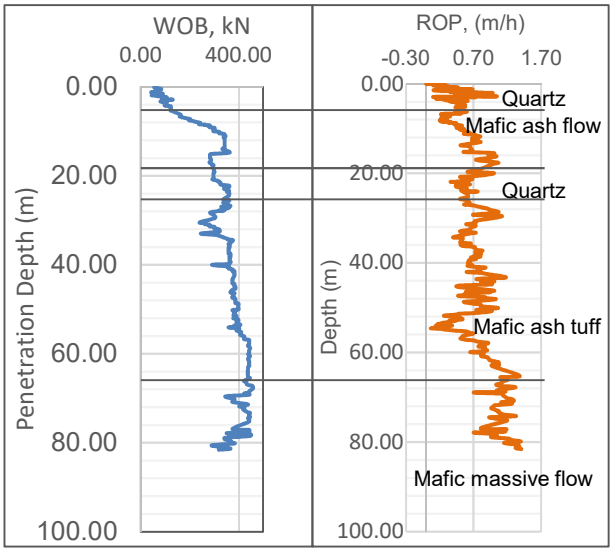


Figure 5. WOB (left) and ROP (right) with depth

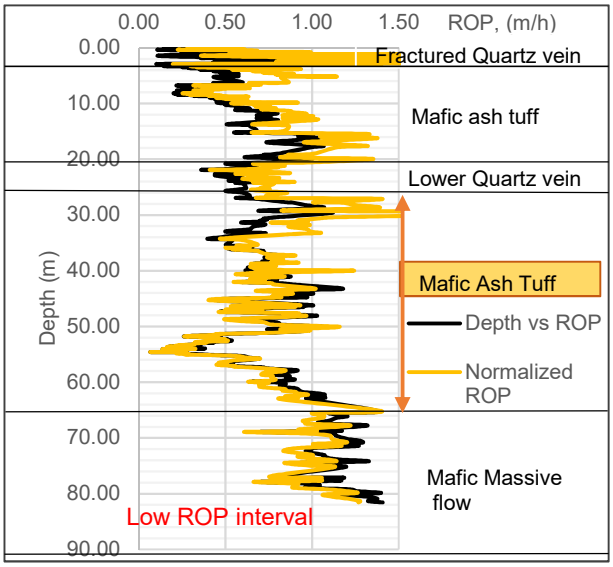


Figure 6. Actual ROP vs Normalized ROP with penetrated depth

Also, in this work, the Maurer model was used to validate the results. Figure 8 shows Maurer ROP with WOB. It is observed that ROP increases with increasing WOB until abnormal low ROP behavior is observed between 50 - 55 m. Also, MSE and DE were analyzed as illustrated in Figure 9.

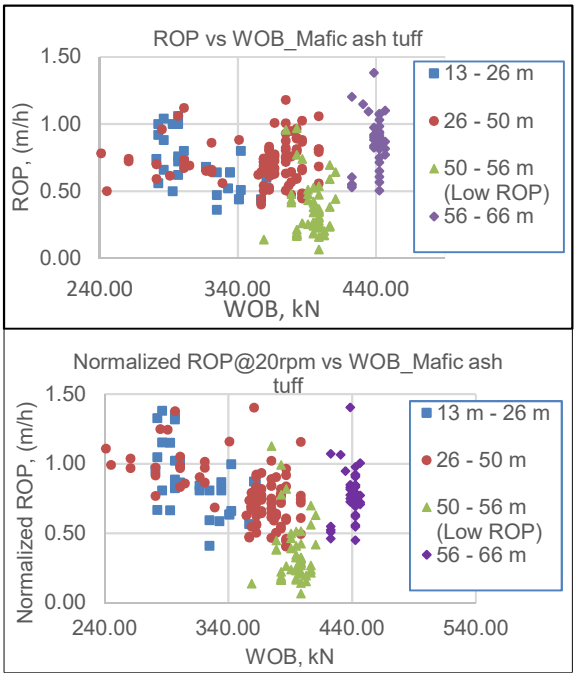


Figure 7.Actual ROP (top) and Normalized ROP (bottom)

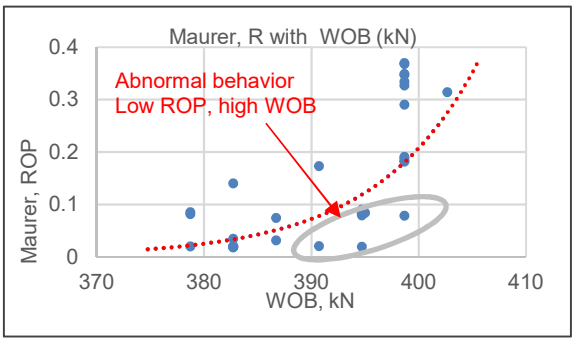


Figure 8. Maurer ROP with WOB the interval between 47m to 60m

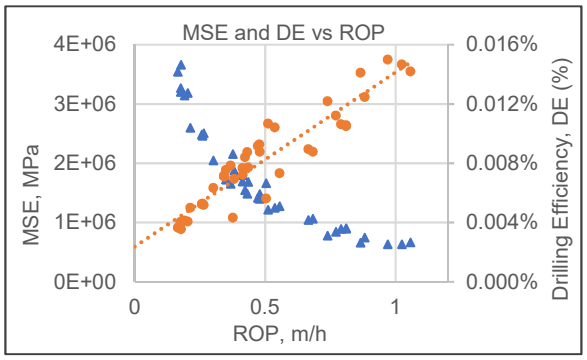


Figure 9. MSE and DE with ROP

## 3.2 Strength and Hardness

### 3.2.1 Unconfined Compressive Strength (UCS)

UCS results were obtained at varying depths within the interval of interest (same lithology of mafic ash tuff). Trends shows UCS values increase as the depth increases. High UCS around 150 MPa is observed between depths of 52 m to 55.3 m, which is the depth interval where lower than expected ROP was observed. See results in Figure 10.

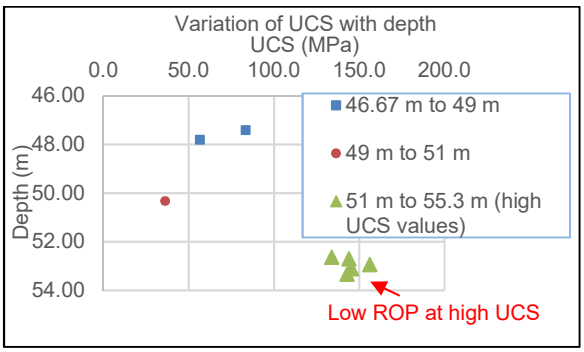


Figure 10. UCS values with penetration depth

### 3.2.2 Point Load Strength Index (PLSI)

The PLSI represents the strength of the intact rock core. Corrected PLSI ($I_{s(50)}$) was calculated from uncorrected ($I_s$) PLSI data and as illustrated (top) in Figure 11, the comparison between both index values is slightly different. Also, in the same Figure 11 (bottom) shows the relationship between corrected PLSI and penetration depth. It is observed that corrected PLSI increases with an increase in penetration depth. Hence, the maximum corrected PLSI in the 52 m to 55.3 m interval is 13 MPa.

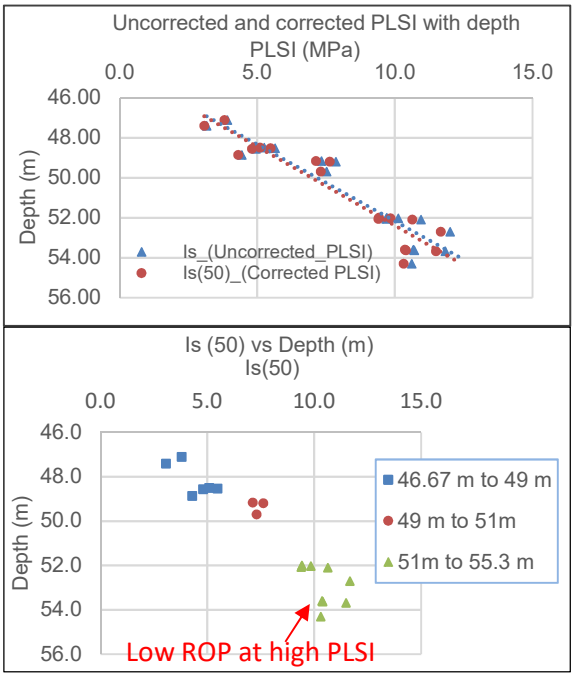


Figure 11. Uncorrected and corrected PLSI (top) and corrected PLSI with penetration depth (bottom)

### 3.2.3 Indirect Tensile Strength (IT)

ITS results with respect to depth are observed to increase with depth. Maximum ITS strength between 20 - 24 MPa is observed at a depth of 54 m as shown in Figure 12.

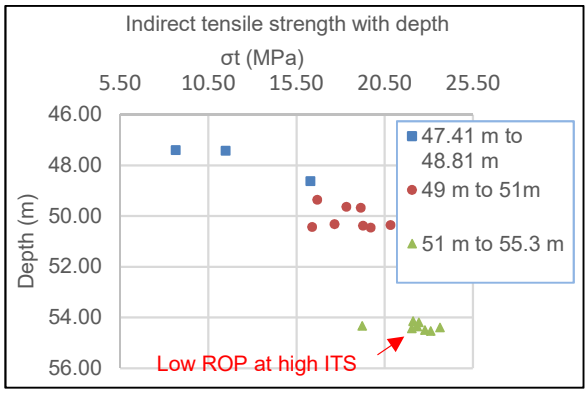


Figure 12. Indirect tensile strength (ITS) with penetration depth

### 3.2.4 Schmidt Hammer (SH)

The hardness of the rock is observed to increase with increased penetration depth (20.7 to 28.0 at 47.41 m to 53.19 m, respectively). Furthermore, the hardness of the rock is observed to be high where there is low ROP (53.2 m) as shown in Table 3.

Table 3. Schmidt Hammer values with penetration depth

| Lithology | Depth (m) | Schmidt Hammer |
|---|---|---|
| Mafic ash tuff with greyish-white color | 47.41 | 20.7 |
| | 50.13 | 22.7 |
| Mafic ash tuff with green-greyish color | 52 | 25.1 |
| | 53.19 | 28 |

### 3.3 Cutting Size Analysis (CSA)

The cutting/grain size distribution curves for cuttings representing the mafic ash tuff lithology were plotted. The interval between 37.6 m - 52.7 m shows the mean size of the particles (D50 values) is between 4 mm and 7.2 mm, as shown in Fig. 13. However, from 53.6 m - 55.6 m, D50 values increased between 6 mm and 10 mm as indicated in Fig. 14.

Grain size parameters such as D90, D60, D50, D30, D10, Coefficient of Curvature (Cc) and Uniformity Coefficient (Cu) were determined. Figure 15 shows that the D50 values increased slightly with an increase of WOB. This observation is to be expected because the particle size of cuttings is getting bigger. However, D90, which represents the 90 percentile by volume of the total particles that is smaller than D90 value, was observed to decrease (abnormality at specified interval) at the lower than expected ROP interval and at approximately 400 kN WOB.

The Cu and Cc were also analyzed. Figure 16 shows the values of Cu and Cc are between 4 to 7 and 0.5 to1, respectively. According to gradation theory, the results indicate the cuttings are well-graded grain size (Holtz & Kovacs, 1981). However, as seen in Figure 16, the curves are steeper between 53.6 m to 55.6 m when compared to the lower interval, which means particles are getting larger with increasing measured depth.

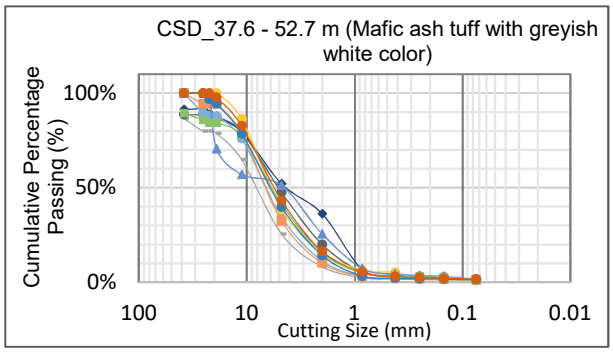


Figure 13. Grain size distribution for the cuttings from 37.6 m to 52.7 m

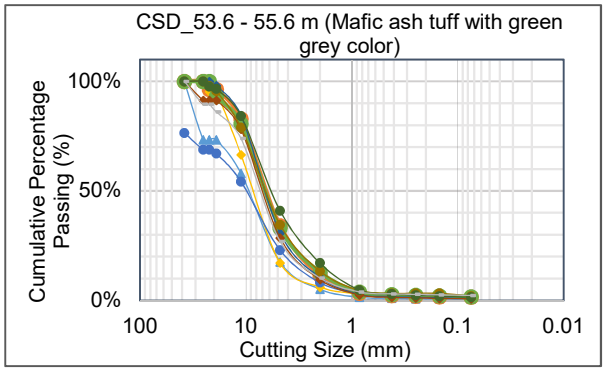


Figure 14. Grain size distribution within low ROP intervals 50 m to 55 m

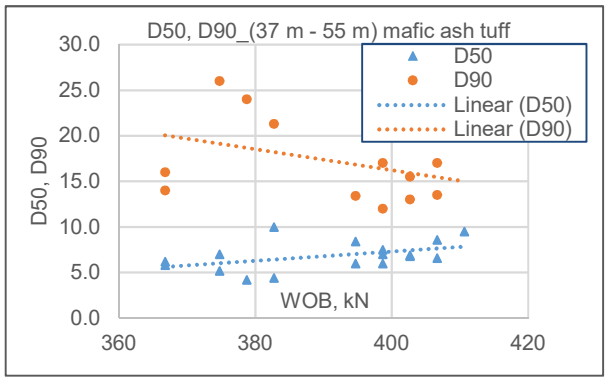


Figure 15. D50 and D90 of the grain size between 37 m to 55 m

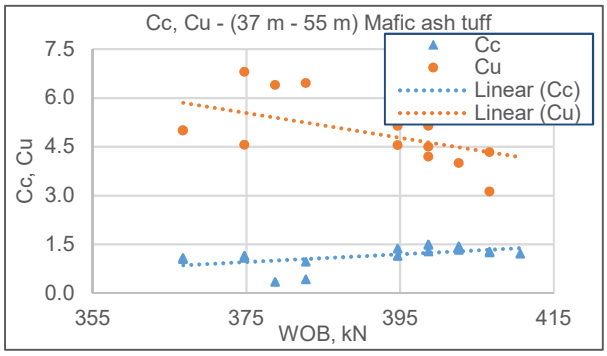


Figure 16. Cc and Cu of the grain size for the interval 37 m to 55 m

### 3.4 Mineral Liberation Analysis (MLA)

MLA tests were conducted on two mafic rock (mafic ash tuff) samples (see Figure 17). One at a measured depth of 43.05 m (above zone of interest) with corresponding expected ROP of 1.09 m/h and another at a depth 54.3 m (at the zone of interest) with a corresponding abnormally low ROP 0.17 m/h. From Table 4, it can be observed that both samples contain a similar overall composition (material balance). However, the grain microstructure varies when comparing both the tested samples (See Figure 18 for mineral composition and grain distribution map). Additionally, the grain structure at 54.03 m (low ROP) shows the presence of accumulated alteration of epidote minerals (see Figure 18). Both of which may have an influence on the increasing strength of the rock and reduced ROP at the interval of interest.

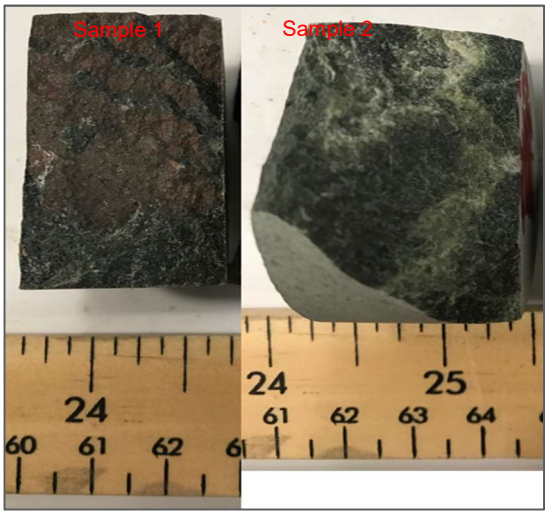


Figure 17. Samples 1 and 2 at 43.05 m and 54.3 m, respectively

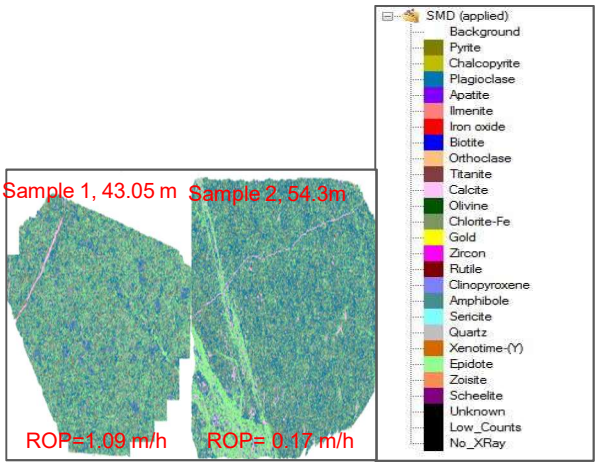


Figure 18. MLA map for samples 1 and 2 (left), legends (right)

Table 4 represents the MLA Weight and Area Composition for each Analyzed Sample

| Minerals | Sample 1 (D = 4 3.05 m) | | Sample 2 (D = 54.3 m) | |
|---|---|---|---|---|
| | Weight % | Area% | Weight% | Area% |
| Total | 100.00 | 100.00 | 100.00 | 100.00 |
| Plagioclase | 21.77 | 24.20 | 23.92 | 26.55 |
| Epidote | 27.62 | 23.89 | 26.07 | 22.52 |
| Chlorite-Fe | 18.52 | 18.42 | 17.30 | 17.19 |
| Quartz | 12.39 | 14.08 | 13.21 | 12.90 |
| Amphibole | 9.75 | 9.54 | 8.51 | 9.66 |
| Orthoclase | 3.85 | 4.49 | 3.40 | 3.96 |
| Titanite | 2.26 | 1.94 | 2.67 | 2.93 |
| Clinopyroxene | 1.97 | 1.73 | 2.38 | 2.04 |
| Calcite | 0.99 | 1.09 | 2.17 | 1.90 |
| Biotite | 0.33 | 0.32 | 0.21 | 0.21 |
| Iron oxide | 0.53 | 0.30 | 0.04 | 0.04 |
| Apatite | 0.01 | 0.01 | 0.00 | 0.00 |
| Others | 0.00 | 0.00 | 0.00 | 0.00 |

## 4 CONCLUSION

This study presents different tests and analyses to investigate the cause of an unexpected low ROP from a LDH field trial. A notable reduction in ROP across a specific measured depth interval of 50 m to 55 m was observed, while at the same time, no notable variation in above and/or below geological lithology was logged and any variation in drilling operation parameters was accounted for. The conclusion can be drawn based on the results:

- The RQD for low ROP interval was found similar as just before interval. Hence, RQD did not give a reasonable conclusion for the occurrence of low ROP at the specified interval.

- The ROP was observed below 0.5 m/h despite an increase of WOB within the interval specified. Actual ROP and normalized ROP are plotted against penetration depth. A decrease in ROP was observed for both cases. The Maurer ROP was plotted and clearly shows the trend of increased ROP when WOB increases, except at a depth of 54 m when WOB is between 390 to 400 kN. Also, it was observed that when MSE increases, both ROP and DE decreases.
- The rock strength for the low ROP interval was higher than just before interval by 150 MPa, 13 MPa and 24 MPa for the UCS, PLSI and ITS respectively. Also, rock hardness increased to 28. Hence, the increase in rock strength and hardness in the low ROP interval is a contributing factor for a decrease in ROP.
- A marginal increase in particle size was observed for the low ROP interval due to the increase in WOB. Also, according to gradation theory, the cuttings are well-graded grain size. However, the D90 values shows a decrease (abnormality trend) with increase of WOB (400 kN), in the low ROP interval.
- MLA showed that variation of mineral grain microstructure may have caused an increase in rock strength and ROP at the depth interval of interest.

## 5 REFERENCES


Abzalov, M. 2016. Diamond Core Drilling. In M. Abzalov, *Modern Approaches in Solid Earth Sciences*, 41-42. WA, Australia: Springer International Publishing Switzerland.

ASTM D3967. 2017. *Standard Test Method for Splitting Tensile Strength of Intact Rock Core Specimens,* Pennsylvania, PA, USA.

ASTM D5731. 2016. *Standard Test Method for Determination of the Point Load Strength Index of Rock and Application to Rock Strength Classifications,* Pennsylvania, PA, USA.

ASTM D5873. 2014. *Standard Test Method for Determination of Rock Hardness by Rebound Hammer Method,* Pennsylvania, PA, USA.

ASTM D6913/6913M. 2017. *Standard Test Methods for Particle-Size Distribution (Gradation) of Soils Using Sieve Analysis,* Pennsylvania, PA, USA.

ASTM D7012. 2014. *Standard Test Methods for Compressive Strength and Elastic Moduli of Intact Rock Core Specimens under Varying States of Stress and Temperatures,* Pennsylvania, PA, USA.

Basu, A., & Aydin, A. 2004. A Method for Normalization of Schmidt Hammer Rebound Values. *International Journal of Rock Mechanics & Mining Sciences*, 41: 1211-1214.

Breeds, C., & Conway, J. J. 1992. Rapid Excavation. In H. L. Hartman, S. G. Britton, D. W. Gentry, M. Karmis, J. M. Mutmansky, W. J. Schlitt, & M. M. Singh, SME *Mining Engineering Handbook 2nd Edition*, 2: 1871-1907. Littleton, Colorado, USA.

Butt, S. D. 2016. Drilling Technology Methods. In M. R. Riazi, *Exploration and Production of Petroleum and Natural Gas*, 197-231. ASTM International.

Cigla, M., Yagiz, M., & Ozdemir, L. 2001. Application of Tunnel Boring Machines in Underground Mine Development. *17th International Mining Congress & Exhibition, Turkey*.

Cumming, J. D., & Smit, J. K. 1980. *In Diamond drill handbook, 3rd Edition*, Toronto.

Holtz, R. D., & Kovacs, W. D. 1981. Grain Size and Grain Size Distribution. In *An Introduction to Geotechnical Engineering*, New Jersey, USA.

Karimi, M. 2013. Drill-Cuttings Analysis for Real-Time Problem Diagnosis and Drilling Performance Optimization. *SPE Asia Pacific Oil & Gas Conference and Exhibition*, Jakarta, Indonesia.

Maurer, W. C. 1962. The "*Perfect-Cleaning*" Theory of Rotary Drilling. *Journal of Petroleum Technology.*

Palmstrom, A. 2005. Measurements of and Correlations between Block Size and Rock Quality Designation (RQD). In W. Broere, S. Li, J. Rostami, & Q. Zhang, *Tunnelling and Underground Space Technology*, 20: 362-377. Norconsult AS, Vestfjordgaten 4, N-1338 Sandvika, Norway.

Pszonka, J., & Sala, D. 2018. Application of the Mineral Liberation Analysis (MLA) for Extraction of Grain Size and Shape Measurements in Siliciclastic Sedimentary Rocks, *4th International Conference on Applied Geophysics,* 02002: 9.

Quan, W., Rasul, G., Abugharara, A., Zhang, Y., Rahman, M. A., & Butt, S. 2021. Empirical Correlations and A new Approach for Strength Evaluation of Isotropic Rocks. *Canadian Geotechnical Society*, Niagara Falls, Ontario, Canada.

Quan, W., Rasul, G., Abugharara, A., Zhang, Y., Rahman, M., & Butt, S. 2021. Tensile and Shear Fracture Examination for Optimal Drilling Performance Evaluation: part-II. *Canadian Geotechnical Society*. Niagara Falls, Ontario, Canada.

Sylvester, P. 2012. Use of the Mineral Liberation Analysis (MLA) for Mineral Logical Studies of Sedimentary Rocks, St. John's, NL.

Teale, R. 1965. The Concept of Specific Energy in Rock Drilling. *International Journal of Rock Mechanics and Mining Sciences & Geomechanics*. 2: 57-73.

Xiao, Y., Zhong, J., Hurich, C., & Butt, S. D. 2015. Micro-Seismic Monitoring of PDC Bit Drilling Performance during Vibration Assisted Rotational Drilling, *49th US Rock Mechanics / Geomechanics Symposium*. San Francisco, CA, USA.

Zhao, K., Gu, S., Yan, Y., Li, Q., Xiao, W., & Liu, G. 2018. Rock Mechanics Characteristics Test and Optimization of High-Efficiency Mining in Dajishan Tungsten Mine, 11, Hindawi.